Accepted Manuscript

An ultrasensitive lysozyme chemiluminescence biosensor based on surface molecular imprinting using ionic liquid modified magetic graphene oxide/β-cyclodextrin as supporting material

Huimin Duan, Xiaojiao Wang, Yanhui Wang, Yuanling Sun, Jianbo Li, Chuannan Luo

PII: S0003-2670(16)30306-3

DOI: 10.1016/j.aca.2016.03.008

Reference: ACA 234458

To appear in: *Analytica Chimica Acta*

Received Date: 3 December 2015

Revised Date: 1 March 2016

Accepted Date: 4 March 2016

Please cite this article as: H. Duan, X. Wang, Y. Wang, Y. Sun, J. Li, C. Luo, An ultrasensitive lysozyme chemiluminescence biosensor based on surface molecular imprinting using ionic liquid modified magetic graphene oxide/β-cyclodextrin as supporting material, *Analytica Chimica Acta* (2016), doi: 10.1016/j.aca.2016.03.008.

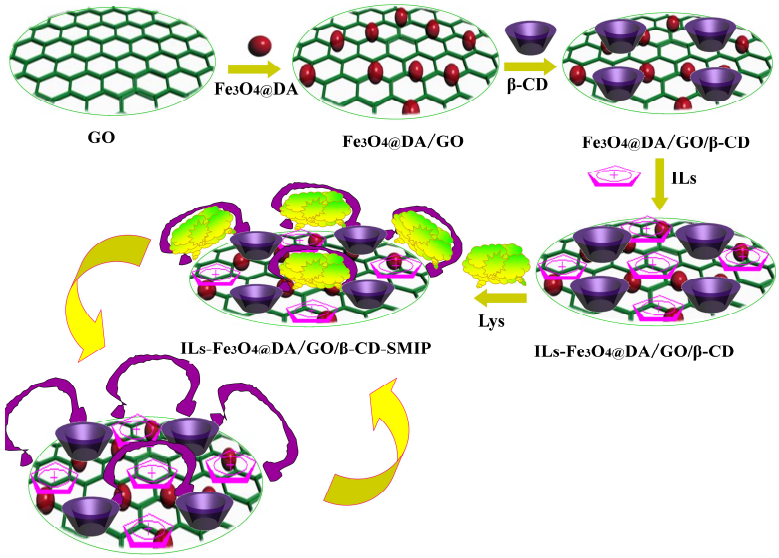

An ultrasensitive lysozyme chemiluminescence biosensor based on surface molecular imprinting using ionic liquid modified magetic graphene oxide/β-cyclodextrin as supporting material

Huimin Duan, Xiaojiao Wang, Yanhui Wang, Yuanling Sun, Jianbo Li, Chuannan Luo*

Key Laboratory of Chemical Sensing & Analysis in Universities of Shandong (University of Jinan), School of Chemistry and Chemical Engineering, University of Jinan, Jinan 250022, China

* Corresponding author. Tel.: +86 0531 89736065. E-mail address: chm_luocn@ujn.edu.cn.

Abstract

In this work, ionic liquid modified Fe_3O_4@dopamine/graphene oxide/ *β*-cyclodextrin (ILs-Fe_3O_4@DA/GO/*β*-CD) was used as supporting material to synthesize surface molecularly imprinted polymer (SMIP) which then was introduced into chemiluminescence (CL) to achieve an ultrasensitive and selective biosensor for determination of lysozyme (Lys). ILs and *β*-CD was applied to provide multiple binding sites to prepare Lys SMIP and Fe_3O_4@DA was designed to make the product separate easily and prevent the aggregation of GO which could improve absorption capacity for its large specific surface area. The ILs-Fe_3O_4@DA/GO/*β*-CD-SMIP showed high adsorption capacity (*Q*=101 mg/g) to Lys in the adsorption isotherm assays. The adsorption equilibrium was reached within 10 min for all the concentrations, attributing to the binding sites situated exclusively at the surface, and the adsorption model followed Langmuir isotherm. Under the suitable CL conditions, the proposed biosensor could response Lys linearly in the range of 1.0×10^{-9} - 8.0×10^{-8} mg/mL with a detection limit of 3.0×10^{-10} mg/mL. When used in practical samples in determination of Lys, the efficient biosensor exhibited excellent result with the recoveries ranging from 94% to112%.

Keywords: ionic liquid; surface molecularly imprinting; lysozyme; chemiluminescence biosensor; *β*-cyclodextrin; Fe_3O_4@dopamine/graphene oxide

1 Introduction

Lysozyme (Lys), widely distributed in body tissues and secretion, was widely applied in food industry as preservative, medical treatment and so on for its bactericidal properties, lytic activation and low molecular weight [1-2]. Hence, the detection of Lys was of considerable importance [3]. There were many methods for determination of Lys containing fluorescence resonance energy transfer [4], aptamer-based biosensor [5], fluorescence [6], electrochemical biosensor [7], and Fe_3O_4@SiO_2@MIPs based CL [8]. Though those methods could offer accurate determination results, some of them were trapped in low selectivity or sensitivity. Chemiluminescence (CL) has attracted considerable attention [9-10] because of its high sensitivity, convenient operation, and had showed high efficiency in determination field.

Molecularly imprinted polymers, with antibody-like binding properties, have shown great promise in molecular sensing [11] and adsorbing [12]. But the eluting of template in imprinting biomacromolecule was incomplete in traditional imprinting technique. Surface molecularly imprinted polymer (SMIP) emerged as the times require [13]. The greatly improved mass transfer and promoted rate of removal of the biomolecule was for the imprinting sites which situated at the surface or close to the surface of the polymer, enabling easy access to the target biomacromolecule [14].

Ionic liquids (ILs) were consisted of ions, and generally composed of organic cations and organic or inorganic anions [15]. As early in 1914, the first ionic liquid-nitro ethylamine was found [16]. The merits of ILs, such as low melting point, good thermal stability, moisture stable and hydrolytic resistance, made the research of

ILs worldwide upsurge, containing development and application [17, 18]. As a new kind of environmentally friendly material, ILs had been widely utilized in many fields [19, 20]. Recently, the general trend was that ILs was used as the functional monomer for preparation of MIP. Yan [21] synthesized ionic liquid molecularly imprinted polymers (ILs-MIP) for application in pipette-tip solid-phase extraction. IL-MIP as adsorbent yielded higher recovery and improved purification efficiency than Si, NH_2, C_{18} and Al_2O_3-N. A novel electrochemical 4-nonyl-phenol sensor with low detection limit based on molecularly imprinted poly (o-phenylenediamine-co-o-toluidine) nitrogen doped graphene nanoribbons ionic liquid composite film was proposed by Pan [22]. Fan used the specific ionic liquid as functional monomer to prepare MIP via precipitation polymerization, which showed a good selectivity and high adsorption capacity for synephrine from methanol-water media [23]. The introduction of ILs in the preparation of MIP made the polymer perform more excellent properties.

Over the years, with various chemically reactive groups such as hydroxyl groups on the basal plane as well as carboxylic acid groups along the sheet edge, graphene oxide (GO) has attracted worldwide attention [24]. Based on the large surface area and good process ability, ILs/GO has attracted increasing interest in many significant fields [25-27]. Recently, of the numerous oxygen-containing functional groups available to form hydrogen bond when synthesizing SMIP, β-CD was widely used as functional molecules [28]. Due to its easy preparation and good biocompatibility, Fe_3O_4 nanoparticles (NPs) were one of the most potential materials and have been widely applied in many fields [29]. Xu promised broad applications of Fe_3O_4 NPs by anchoring dopamine (Fe_3O_4@DA) to immobilize functional molecules on the surface of Fe_3O_4 NPs [30]. DA could not only prevent the aggregation of Fe_3O_4 dispersion but also reduce the toxicity and oxidation of Fe_3O_4. On the other hand，DA possessed

abundant hydroxyl and amino groups that could be used for further modification.

In this study, a new material ILs-Fe_3O_4@DA/GO/*β*-CD was synthesized. In the new material, Fe_3O_4@DA was used to make the polymer separate easily. ILs, GO and *β*-CD were introduced to serve as backbone material and improve the mass transfer as functional monomer in the preparation of SMIP. Then, ILs-Fe_3O_4@DA/GO/*β*-CD-SMIP exhibited excellent recognition and adsorption ability to Lys owing to the imprinting cavities situated at the surface of the material's surface. Finally, an ultrasensitive and selective CL biosensor for determination of Lys was proposed based on ILs-Fe_3O_4@DA/GO/*β*-CD-SMIP.

2 Experiments

2.1 Chemicals and materials

Lys, *β*-cyclodextrin (*β*-CD, 96%), and Ammonium persulphate (APS, AR) were supplied by Sinopharm Chemical Reagent Co. Ltd (China); 3-Bromopropylamine hydrobromide (79%), N,N,N',N'-tetramethyl ethylenediamine (TEMED, A.R), Dimethylaminoethyl acrylate (DMAEMA, 99%), and 4-Amino-5-imidazolecarboxamide hydrochloride (98%) were purchased from Aladdin Industrial Co. (China); Potassium permanganate, Acetic acid, Methanol, Luminol and all the other chemicals unless specified were of analytical reagent grade and used without further purification. Phosphate buffer solution (PBS, pH = 6.5, 0.01 mol/L) solution was used in all the experiment and stored in refrigerator (4°C).

2.2 Apparatus

The IFFM-E flow injection CL analyser (Xi'an Remex Electronic instrument High-Tech Ltd., China) was equipped with an automatic injection system and a detection system. A certain amount of ILs-Fe_3O_4@DA/GO/*β*-CD-SMIP and non-imprinting polymer (ILs-Fe_3O_4@DA/GO/*β*-CD-SNIP) was placed in front of the CL

analyser shown in Fig 1. XRD measurement was made on a D8 focus spectrometer (Brooke AXS, Germany). The morphology of nanoparticles was analyzed with a scanning electron microscope (SEM, GUANTA FEG 250, America).

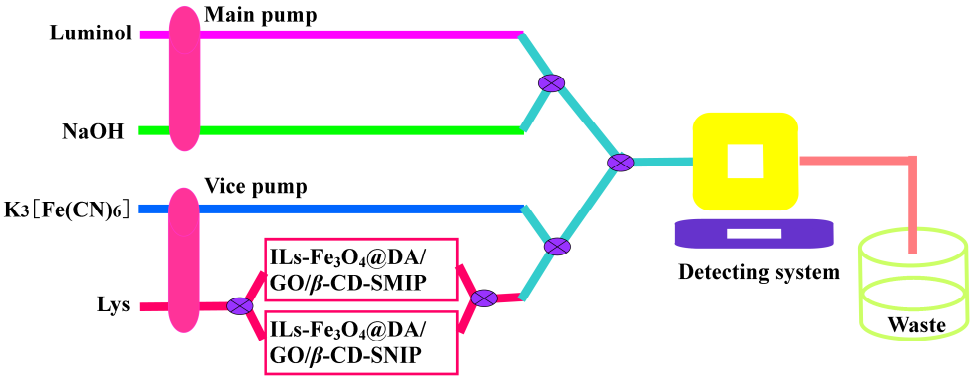

Fig. 1 Schematic diagram of Lys ILs-Fe_3O_4@DA/GO/β-CD -SMIP-CL biosensor

2.3 Preparation of Fe_3O_4@DA/GO

GO was prepared from nature graphite powders by a modified Hummers method and our group [31]. Briefly, 100 mL of H_2SO_4 was added into a 500 mL flask followed by adding 3.0 g of graphite powder. Then, 15 g of $KMnO_4$ was subsequently added. The diluted suspension was stirred at 98°C, followed by addition of 30% H_2O_2. Finally, the mixture was filtered and washed till the pH = 7.0. Fe_3O_4@DA/GO was synthesized according to a modified procedure in our group and previous literatures [30, 31]. By suspending 0.5 g GO in 200 mL of solution containing 1.7 g $(NH_4)_2Fe(SO_4)_2 \cdot 6H_2O$ and 2.51 g $NH_4Fe(SO_4)_2 \cdot 12H_2O$ under N_2 atmosphere, the solution was sonicated. Then, 10 mL of 8 mol/L NH_4OH aqueous solutions was added till the pH = 11.5. Then, 5 mL acetic acid was injected into the solution and the black precipitation was separated with an external magnetic field, and washed, and then dried. Subsequently, 50 mg of dopamine hydrochloride was dissolved in 200 mL pH = 4.0 solution. 50 mg as prepared nanoparticles was then added and stirred. Fe_3O_4@DA/GO was collected, washed with water, and dried.

2.4 Preparation of Fe_3O_4@DA/GO/*β*-CD

By suspending 0.2 g of chitosan in 40 mL of 2% acetic acid by ultrasonication, 0.1 g Fe_3O_4@DA/GO and 80 mg *β*-CD were added to the molten chitosan colloidal solution, and stirred for 1 h. 30 mL NH_3H_2O and 1mL hydrazine hydrate was added in above solution by stirring. Then, 6 mL 25% glutaraldehyde was added to the mixed solution. After the solution was stirred, 1 mol/L sodium hydroxide was added till the pH=10.5. The reaction was carried out under constant mechanical stirring. The precipitate was isolated in the magnetic field and washed with water and isolated by a permanent magnet. The obtained composites were then dried under vacuum.

2.5 Preparation of ILs-Fe_3O_4@DA/GO/*β*-CD

1.6258 g 4-amino-5-imidazolecarboxamide was added to 10 mL of anhydrous ethanol. Then, 2.1892 g 3-bromopropylamine hydrobromide was dissolved in 20 mL of anhydrous ethanol and was added dropwise with the protection of N_2. Viscous liquid was collected by suction filtration and vacuum drying. Subsequently, 1 mL of ILs dissolved in methanol was well-distributed in 100 mg Fe_3O_4@DA/GO/*β*-CD dissolved in anhydrous methanol. After agitation, the product was separated and dried.

2.6 Preparation of ILs-Fe_3O_4@DA/GO/*β*-CD-SMIP

ILs-Fe_3O_4@DA/GO/*β*-CD-SMIP was synthesized according to a modified procedure described in our work and previous literature [32], and the preparing process as presented in Fig. 2. The preparing process was shown in Fig. 2. MA (32 mg) and DMAEMA (0.2 mL) were dissolved in PBS solution and mixed thoroughly. 32 mg of Lys was dissolved to the solution by ultrasonication. Then, 150 mg ILs-Fe_3O_4@DA/GO/*β*-CD dispersed in 15 mL ethanol and 5 mL PBS solution was added into above solution. Subsequently, the solution was shaked to preassemble. By adding 30 mg of APS and 0.4 mL TEMED to the mixture, polymerization was

initiated and continued. After the polymerization, the Lys-imprinting particles were collected. The particles were washed with water and then repeatedly with certain concentration of NaCl solution. Finally, they were washed with PBS solution. The ILs-Fe_3O_4@DA/GO/*β*-CD-SMIP was dried for further use. The ILs-Fe_3O_4@DA/GO/*β*-CD-SNIP was prepared by adding PBS solution instead of Lys solution while the other steps were the same.

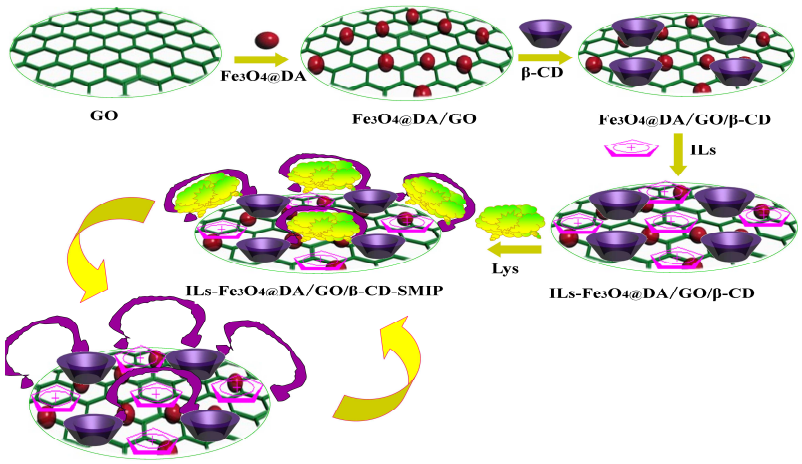

Fig.2. The preparing process of Lys ILs-Fe_3O_4@DA/GO/*β*-CD-SMIP

2.7 Adsorbing performance of ILs-Fe_3O_4@DA/GO/*β*-CD-SMIP and ILs-Fe_3O_4@DA/GO/*β*-CD-SNIP

Adsorption experiments: 50 mg ILs-Fe_3O_4@DA/GO/*β*-CD-SMIP and ILs-Fe_3O_4@DA/GO/*β*-CD-SNIP nanoparticles were placed into 5 mL centrifuge tubes, respectively. Then, 2.0 mL of different concentration solution of Lys was added into the tube and the dispersion liquid was shaked. After separation, the concentration of the supernatant in the tube was determined by CL instrument. Rebinding dynamics: 50 mg ILs-Fe_3O_4@DA/GO/*β*-CD-SMIP and ILs-Fe_3O_4@DA/GO/*β*-CD-SNIP NPs were dispersed in 2.0 mL 2.0 mg/mL Lys solution which then was shaked for 1 min, 5 min, 10 min, 15 min, 20 min, 25 min and 30 min respectively. After separation, the concentration of the supernatant in the tube was determined by CL instrument.

The amount of Lys adsorbed by the particles was calculated by formula (1).

$$Q = \frac{(c_0 - c_e)V}{m} \quad (1)$$

Where Q (mg/g) was the mass of Lys adsorbed by unit mass of dry particles, c_0 (mg/mL) and c_e (mg/mL) were the concentrations of Lys in the initial and final solutions, respectively, V (mL) was the volume of the adsorption mixture, and m (g) was the mass of the ILs-Fe_3O_4@DA/GO/*β*-CD-SMIP.

3 Results and discussion

3.1 Characterization of ILs-Fe_3O_4@DA/GO/*β*-CD-SMIP

The results of SEM characterization of the prepared GO nanosheets and Fe_3O_4@DA/GO nanoparticles were shown in Fig. 3. The synthesized GO nanosheets (Fig. 3 A) had lateral dimensions of several micrometers and large surface areas, and the straticulate single layered GO was formed with wrinkle in the edge exactly. From the SEM image (Fig. 3 B) of the Fe_3O_4@DA/GO nanoparticles, it could be seen clearly that GO sheets were the matrix of Fe_3O_4@DA nanoparticles and the Fe_3O_4@DA nanoparticles were disorderly distributed on the surface of GO, and no wrinkles were observed on the surface of the GO composite, which confirmed that the loading of Fe_3O_4@DA was important for preventing aggregation of GO. As shown in Fig. 3 C, the morphology of ILs-Fe_3O_4@DA/GO/*β*-CD-SMIP was observed, where a regularly rough imprinting polymer overlayed on the surface of ILs-Fe_3O_4@DA/GO/*β*-CD. The greatly different surface appearance of SMIP and SNIP confirmed the successful fabrication of SMIP.

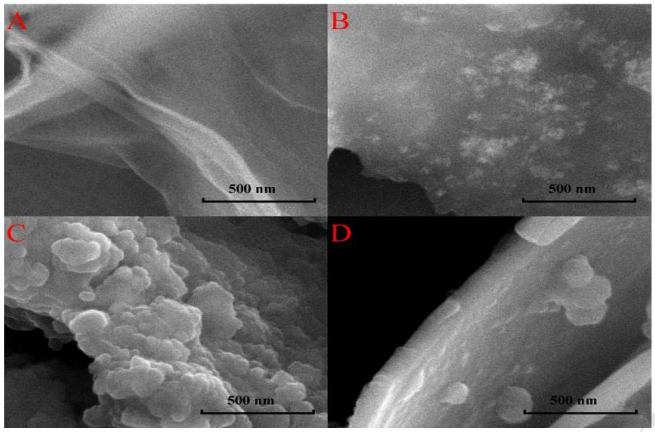

Fig.3. The SEM images of GO (A), Fe_3O_4@DA/GO nanoparticles (B), ILs-Fe_3O_4@DA/GO/*β*-CD-SMIP (C) and ILs-Fe_3O_4@DA/GO/*β*-CD-SNIP (D)

3.2 Adsorption performance of ILs-Fe_3O_4@DA/GO/*β*-CD-SMIP and ILs-Fe_3O_4@DA/GO/*β*-CD-SNIP

Fig. 4 clearly showed the adsorption capacity of Lys onto the ILs-Fe_3O_4@DA/GO/*β*-CD-SMIP. Batch adsorption experiments (Fig. 4 A): In general, the adsorption process was dependent on the initial Lys concentrations. With the increase in initial concentration from 0.1 to 2.0 mg/mL, the amount of Lys adsorbed increased evidently. And with the increase in the initial concentration, the driving force of concentration gradient to overcome the mass transfer resistance of the Lys molecules between the aqueous phases and the solid phases increased. As a result, the absorption ability of ILs-Fe_3O_4@DA/GO/*β*-CD-SMIP was found to be 101 mg/g. Rebinding kinetics (Fig. 4 B): On the other hand, for the adequate free adsorptive sites and a high concentration of Lys, the adsorption proceeded rapidly with the contact time. Thereafter, the adsorption rates were considerably slowly and equilibrium was reached within 10 min for all the concentrations, attributing to the binding sites situated exclusively at the surface.

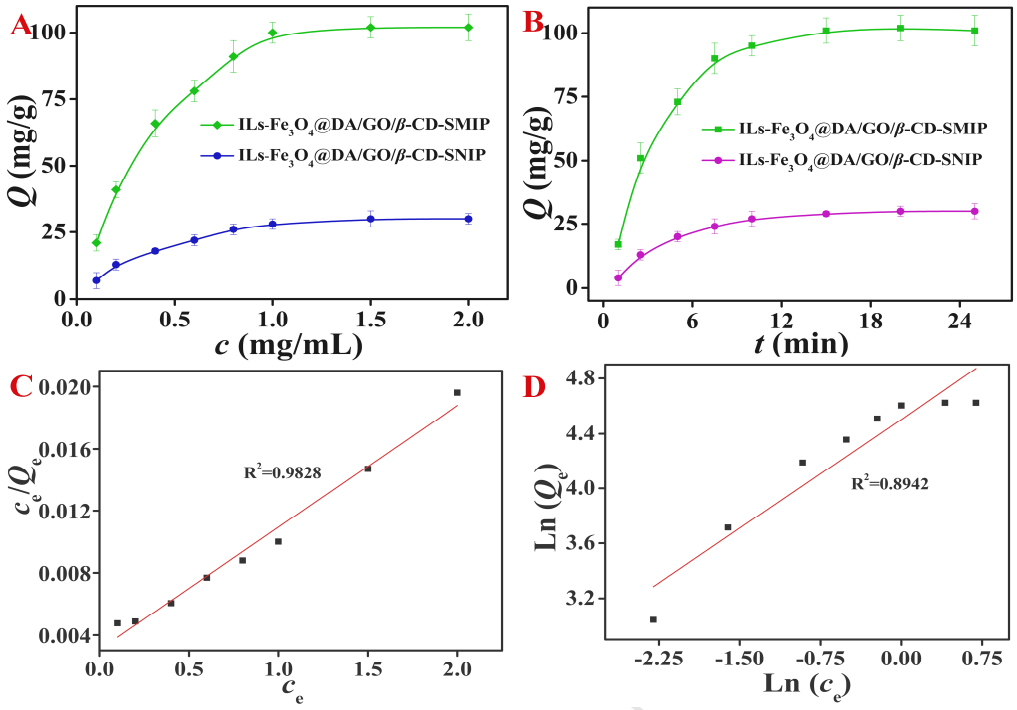

Fig.4. Adsorption isotherm curves (A), kinetics curves (B), Langmuir adsorption isotherm fit (C) and Freundlich adsorption isotherm fit (D) of ILs-Fe_3O_4@DA/GO/*β*-CD-SMIP

The Langmuir and Freundlich equations were used for modeling adsorption isotherms, respectively. As shown in Fig. 4 C D, the linear fitting curves of the Langmuir and Freundlich models indicated that the Langmuir isotherm was more appropriate than the Freundlich model for the relative standard deviation values. The results revealed that the energy on the surface of ILs-Fe_3O_4@DA/GO/*β*-CD-SMIP was the same and correspondingly adsorption process was mainly monolayer uniform adsorption. Therefore, it certificated that the imprinting cavies were on the surface of ILs-Fe_3O_4@DA/GO/*β*-CD-SMIP, which enabled easy access to the Lys.

3.3 Extraction condition and adsorption pH

Extraction condition: To reuse the ILs-Fe_3O_4@DA/GO/*β*-CD-SMIP, a washing step was required to remove the Lys without desorbing the imprinted cavities in ILs-Fe_3O_4@DA/GO/*β*-CD-SMIP. For the large number of complex matrix components in the biological samples, different concentrations of NaCl were

evaluated as washing solvent to obtain better pre-concentration efficiency. Fig 5 (A) showed that ILs-Fe_3O_4@DA/GO/β-CD-SMIP exhibited a higher binding capacity toward template when the NaCl concentration was 0.04 mol/L. Thus, Lys could be efficiently eluted off ILs-Fe_3O_4@DA/GO/β-CD-SMIP with 0.04 mol/L of NaCl.

Adsorption pH: As rebinding solution, pH of PBS solution was studied over the range of 6.0-7.5 and the results was shown in Fig 5 (B). It showed that when pH = 6.5, the amount of Lys adsorbed on ILs-Fe_3O_4@DA/GO/β-CD-SMIP reached maximum with a significant decrease at lower or higher pH values. The reason maybe was that the primary driving forces for the rebinding process, such as hydrogen, electrostatic and hydrophobic bonding, were strongly related to the ionization states of amino acid side chains and the conformational state of Lys molecules which might be more suitable for the imprinted cavities when pH=6.5 [32].

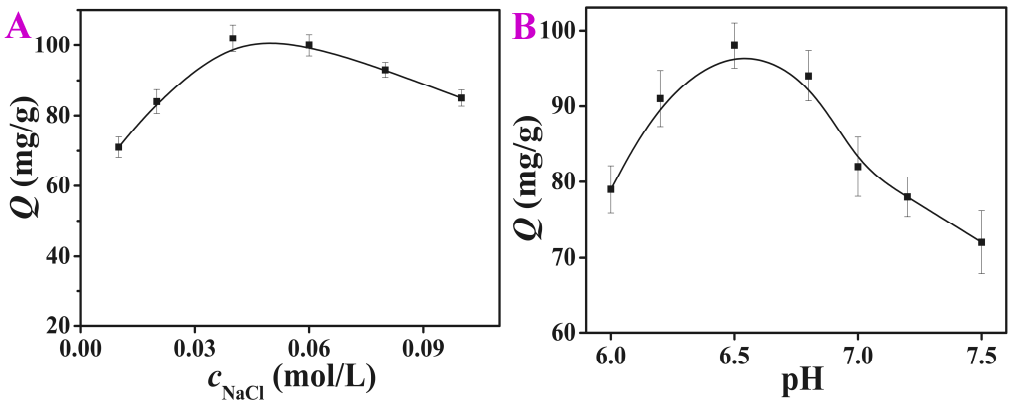

Fig.5. Effect of concentration of NaCl on the extraction process (A) and the effect of pH of phosphate buffer on the adsorption process (B)

3.4 Optimization of analytical conditions the CL biosensor

The adsorption time which depended on peristaltic pumps speed was an important parameter for the amount of Lys in the solution or absorbed on the ILs-Fe_3O_4@DA/GO/β-CD-SMIP. When pumps speed was too high, Lys molecules could not be absorbed by ILs-Fe_3O_4@DA/GO/β-CD-SMIP completely. And when

pumps speed was too low, the other substances in the samples would be absorbed by ILs-Fe_3O_4@DA/GO/*β*-CD-SMIP. Thus, 30 rpm for main pump speed and 25 rpm for vice pump speed were optimized between 20-40 rpm for further work.

The concentrations of NaOH, luminol and $K_3[Fe(CN)_6]$ would affect the CL intensity, and were chosen as showed in Fig. 6 ABC. In which, ΔI was the CL signal difference between the solution containing Lys and the blank solution. As could be seen that the maximum CL intensity could be obtained at the concentration of $K_3[Fe(CN)_6]$: 2.0 × 10^{-3} mol/L, NaOH: 0.1 mol/L, and luminol: 3.0 × 10^{-5} mol/L simultaneously.

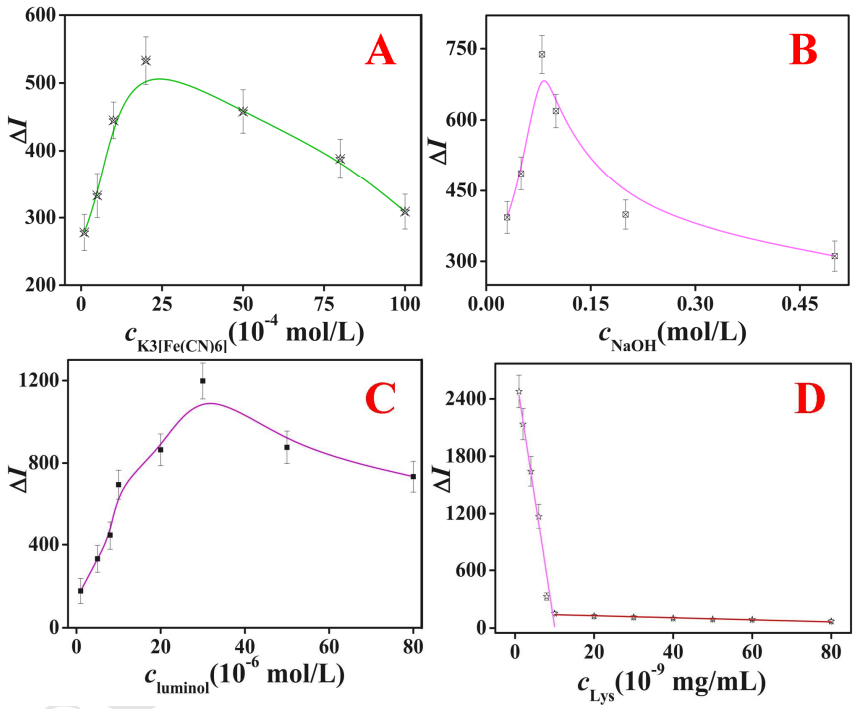

Fig.6. Optimization results: Effect of $K_3[Fe(CN)_6]$ (A), NaOH (B) and luminol (C) concentration on CL intensity; Regression equation of the ILs-Fe_3O_4@DA/GO/*β*-CD-SMIP-CL biosensor (D)

3.5 Analytical performance of ILs-Fe_3O_4@DA/GO/*β*-CD-SMIP-CL biosensor

In this work, with the addition of Lys into the luminol, $K_3[Fe(CN)_6]$ and NaOH solutions, an amplified CL signal was observed. For its favorable characteristics of high selectivity and stability, ILs-Fe_3O_4@DA/GO/*β*-CD-SMIP could contribute to

higher accuracy and lower detection limit for the template-monomer complex [33]. Under the optimal experimental conditions described above (c(NaOH) = 0.1 mol/L, c(luminol) = 3.0×10^{-5} mol/L and $c(K_3[Fe(CN)_6])$ = 2.0×10^{-3} mol/L), the amplified CL intensity presented a good linearity with the concentration of Lys in the range of 1.0×10^{-9} - 8.0×10^{-8} mg/mL with a detection limit of 3.0×10^{-10} mg/mL (3δ) which was compared with traditional methods shown in Tab. 1 and the results were satisfied. The regression equation shown in Fig. 6 D was divided into two parts: (1.0×10^{-9} - 1.0×10^{-8} mg/mL) $\Delta I = 2708 - 269 \times 10^{9}\ c$ (c: mg/mL) with a correlation coefficient of 0.9912 and (1.0×10^{-8} - 8.0×10^{-8} mg/mL) $\Delta I = 151 - 1.1 \times 10^{9}\ c$ (c: mg/mL) with a correlation coefficient of 0.9915.

Tab.1. Comparing results with conventional methods

Methods	Liner Range (mg/mL)	Detection Limit (mg/mL)
Our work	1.0×10^{-9} - 8.0×10^{-8}	3.0×10^{-10}
Fluorescence resonance energy transfer [4]	0 - 39.7×10^{-3}	0.80×10^{-3}
Aptamer-Based Biosensors [5]	0.5×10^{-3}- 50×10^{-3}	0.2×10^{-3}
Fluorescence [6]	0×10^{-6} - 15×10^{-6}	2.86×10^{-6}
Electrochemical biosensor [7]	5×10^{-8} - 1.0×10^{-4}	1.5×10^{-8}
Fe_3O_4@SiO_2@MIPs-CL [8]	5×10^{-6}- 2.0×10^{-3}	5×10^{-6}

3.6 Selectivity studies of the biosensor

Fig. 7 A showed the adsorption capacities of the ILs-Fe_3O_4@DA/GO/β-CD-SMIP and ILs-Fe_3O_4@DA/GO/β-CD-SNIP particles to four proteins in PBS solutions and some other amino acid such as tryptophan, cysteine and fydroxyproline. Compared with both ILs-Fe_3O_4@DA/GO/β-CD-SMIP and ILs-Fe_3O_4@DA/GO/β-CD-SNIP particles, the imprinted particles exhibited much higher binding amounts for Lys. To evaluate the selectivity of the imprinted biosensor,

different analytes with increasing amounts were added in standard Lys solution involving Horseradish Peroxidase (HRP), bovine serum albumin (BSA), bovine hemoglobin (BHb), Uric Acid, Lemon Acid, Ca^{2+}, Hydroxyproline and ribonuclease A (RNase A), respectively. In the CL system, 50 times BSA concentration (compared with Lys) interfered with the determination of Lys but when using ILs-Fe_3O_4@DA/GO/*β*-CD-SMIP, 100 times BSA concentration would interfere with the determination of Lys for the imprinting cavities which were suitable for macromolecule and could recognize and absorb Lys specifically. Similarly, interferences from HRP, Uric Acid, Lemon Acid, Ca^{2+}, Hydroxyproline, RNase A and BHb, which were existed in human urine, were investigated and shown in Fig. 7 B.

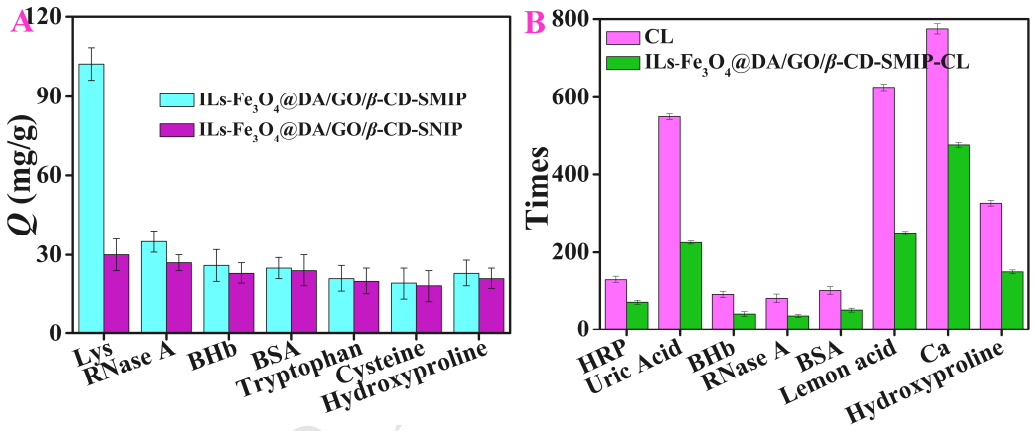

Fig.7. Binding amounts of different proteins on the imprinted particles (A); Interferences study of the ILs-Fe_3O_4@DA/GO/*β*-CD-SMIP-CL biosensor (B)

3.7 Reusability of the ILs-Fe_3O_4@DA/GO/*β*-CD-SMIP

Under the extraction condition, Lys in ILs-Fe_3O_4@DA/GO/*β*-CD-SMIP was extracted for adsorption again. The adsorption capacity of used ILs-Fe_3O_4@DA/GO/*β*-CD-SMIP could be obtained and then compared with the adsorption capacity of ILs-Fe_3O_4@DA/GO/*β*-CD-SMIP before any use. The result showed that there was 10% adsorption capacity loss within 4 times of ILs-Fe_3O_4@DA/GO/*β*-CD-SMIP to the concentration of 1.0×10^{-8} mg/mL Lys, which

powerfully demonstrated that the ILs-Fe_3O_4@DA/GO/*β*-CD-SMIP was excellently reusable in the detection of Lys.

3.8 Application of the ILs-Fe_3O_4@DA/GO/*β*-CD-SMIP-CL biosensor

In this study, the feasibility of the biosensor for human urine applications was investigated as shown in Tab.2. Under optimal experimental conditions, the recoveries ranged from 94% to 112%. Obviously, these results were satisfactory and showed that the biosensor was precise with good accuracy. Therefore, it was entirely feasible to say that the efficient ILs-Fe_3O_4@DA/GO/*β*-CD-SMIP-CL biosensor could be used in the detection of Lys in human urine.

Tab.2. Assay of Lys in human urine by means of ILs-Fe_3O_4@DA/GO/*β*-CD-SMIP-CL biosensor

Sample	Found in serum (10^{-9} mg/mL)	Added amount (10^{-9} mg/mL)	Found amount (n=6) (10^{-9} mg/mL)	RSD%	Recovery (%)
Urine 1	3.5	2.5	6.2	4.5	108
		5.0	8.2	4.7	94
Urine 2	3.7	2.5	6.5	4.3	112
		5.0	8.8	3.9	102

4 Conclusion

In this work, a sensitive and selective CL biosensor for the determination of Lys was achieved based on ILs-Fe_3O_4@DA/GO/*β*-CD-SMIP. ILs and *β*-CD was applied to provide multiple binding sites to prepare Lys SMIP and Fe_3O_4@DA was designed to make the product separate easily and prevent the aggregation of GO which could improve absorption capacity for its large specific surface area. The ILs-Fe_3O_4@DA/GO/*β*-CD-SMIP showed high adsorption capacity to Lys in the adsorption isotherm assays. One of the most important considerations of the efficient biosensor was a profound understanding of application of multifunctional material,

which imparted specific analytical performance to the biosensor, as well as to improve the reusability and mechanical stability. At the same time, the efficient ILs-Fe_3O_4@DA/GO/*β*-CD-SMIP-CL biosensor exhibited excellent ultra sensitivity, selectivity and accuracy when used to determine Lys in practical samples.

Acknowledgements

This work was supported by the Shandong Provincial Natural Science Foundation of China (No. ZR2012BM020).

Reference

[1] R. Swaminathan, V.K. Ravi, S. Kumar, M.V.S. Kumar, N. Chandra, Lysozyme: A model protein for amyloid research, Adv. Pro. Chem. Str. Bio. 84 (2011) 63-111.

[2] C. Corradini, I. Alfieri, A. Cavazza, C. Lantano, N. Zucchetto, A. Montenero, Antimicrobial films containing lysozyme for active packaging obtained by sol-gel technique, J. Food Eng. 119 (2013) 580-587.

[3] S. Wang, T. Bung, T. Chen, D. Lin, J. Wu, P. Rao, X. Ye, First report of a novel plantlysozyme with both antifungal and antibacterial activities, Biochem. Biophys. Res. Commun. 327 (2005) 820-827.

[4] J. Wang, B. Liu, Fluorescence resonance energy transfer between an anionic conjugated polymer and a dye-labeled lysozymeaptamer for specific lysozyme detection, Chem. Commun. 17 (2009) 2284-2286.

[5] A.K.H. Cheng, B. Ge, H.Z. Yu, Aptamer-based biosensors for label-free voltammetric detection of lysozyme, Anal. Chem. 79 (2007) 5158-5164,

[6] D. Tang, D. Liao, Q. Zhu, F. Wang, H. Jiao, C. Yu, Fluorescence turn-on detection of a protein through the displaced single-stranded DNA binding protein binding to a molecular beacon, Chem, Commun, 47 (2011) 5485-5487.

[7] Z. Zhang, S. Zhang, L. He, D. Peng, F. Yan, H. Zhang, S. Fang, Feasible electrochemical biosensor based on plasma polymerizationassisted composite of polyacrylic acid and hollow TiO_2 spheres for sensitively detecting lysozyme, Biosens. Bioelectron. 74 (2015) 384-390.

[8] T. Jing, H. Du, Q. Dai, H. Xia, S. Mei, Y. Zhou, Magnetic molecularly imprinted nanoparticles for recognition of lysozyme, Biosens. Bioelectron. 26 (2010) 301-306.

[9] J.M. Parka, H.W. Jung, Y.W. Chang, H.S. Kim, M.J. Kang, J.C. Pyun,

Chemiluminescence lateral flow immunoassay based on Pt nanoparticle with peroxidase activity, Anal. Chim. Acta. 853 (2015) 360-367.

[10] C. Ding, Z. Wang, H. Zhong, S. Zhang, Ultrasensitive chemiluminescence quantification of single-nucleotide polymorphisms by using monobase-modified Au and CuS nanoparticles, Biosens. Bioelectron. 25 (2010) 1082-1087.

[11] H. Li, C. Xie, X. Fu, Electrochemiluminescence sensor for sulfonylurea herbicide with molecular imprinting core-shell nanoparticles/chitosan composite film modified glassy carbon electrode, Sensor. Actuator. B 181 (2013) 858-866.

[12] J. Pan, Y. Yin, M. Gan, M. Meng, X. Dai, Y. Yan, Fabrication and evaluation of molecularly imprinted multi-hollow microspheres adsorbents with tunable inner pore structures derived from templating Pickering double emulsions, Chem. Eng. J. 266 (2015) 299-308.

[13] K. Dabulis, A.M. Klibanov, Molecular imprinting of proteins and other macromolecules resulting in new adsorbents, Biotechnol. Bioeng. 39 (1992) 176-185.

[14] M. Kempe, M. Glad, K. Mosbach. An approach towards surface imprinting using the enzyme ribonuclease A, J. Mol. Recognit. 8 (1995) 35-39.

[15] K.R. Seddon, Ionic liquids for clean technology. J. Chem. Tec. Biotec. 68 (1997) 351-356.

[16] S. Sugden, H.J. Wilkins, CLXVII.-The parachor and chemical constitution.Part XII.Fused metals and salts, J. Chem. Soc. 0 (1929) 1291-1298.

[17] M. Armand, Frank Endres, D.R. MacFarlane, H. Ohno, B. Scrosati, Ionic-liquid materials for the electrochemical challenges of the future, Nature Mater. 8 (2009) 621-629.

[18] E.E. Fileti, V.V. Chaban, Imidazolium ionic liquid helps to disperse fullerenes in

water, J. Phys. Chem. Lett.. 5 (2014) 1795-1800.

[19] R.D. Rogers, K.R. Seddon, Ionic Liquids-Solvents of the Future? Science, 2003, 302: 792-793.

[20] J. Yang, L. Zhou, X. Guo, L. Li, P. Zhang, R. Hong, T. Qiu, Study on the esterification for ethylene glycol diacetate using supported ionic liquids as catalyst: Catalysts preparation, characterization, and reaction kinetics, process, Chem. Eng. J. 280

[21] H. Yan, C. Yang, Y. Sun, K.H. Row, Ionic liquid molecularly imprinted polymers for application in pipette-tip solid-phase extraction coupled with gas chromatography for rapid screening of dicofol in celery, J. Chromatogr. A 1361 (2014) 53-59.

[22] Y. Pan, L. Shang, F. Zhao, B. Zeng, A novel electrochemical 4-nonyl-phenol sensor based on molecularly imprinted poly (o-phenylenediamine-co-o-toluidine)-nitrogen-doped graphene nanoribbons-ionic liquid composite film, Electrochim. Acta 151 (2015) 42

[23] J.P. Fan, Z.Y. Tian, S. Tong, X.H. Zhang, X.K. Ouyang, A novel molecularly imprinted polymer of the specific ionic liquid monomer for selective separation of synephrine from methanol-water media, Food Chem. 141 (2013) 3578-3585.

[24] J. Jagiello, J. Judek, M. Zdrojek, M. Aksienionek, L. Lipinska, Production of graphene composite by direct graphite exfoliation with chitosan, Mater. Chem. Phys. 148 (2014) 507-511.

[25] B. Lin, H. Shang, F. Chu, Y. Ren, Y. Wei, J. Ding, Ionic liquid-tethered graphene oxide/ionic liquid electrolytes for highly efficient dye sensitized solar cells, Electrochim. Acta 134 (2104) 209-214.

[26] P. Zhao, J. Hao, 2,6-Diaminopyridine-imprinted polymer and its potency to

hair-dye assay using graphene/ionic liquid electrochemical sensor, Biosens. Bioelectron. 64 (2015) 277-284.

[27] H.K.S.V. Mohan, J. An, K. Liao, C.H. Wong, L. Zheng, Detection and classification of host–guest interactions using β-cyclodextrin-decorated carbon nanotube-based chemiresistors, Curr. Appl. Phys. 14 (2014) 1649-1658.

[28] J. Pan, X. Zou, X. Wang, W. Guan, Y. Yan, J. Han, Selective recognition of 2,4-dichlorophenol from aqueous solution by uniformly sized molecularly imprinted microspheres with β-cyclodextrin/attapulgite composites as support, Chem. Eng. J. 162 (2010) 910-918.

[29] Y. Zhang, Y. Li, Y. Hu, G. Li, Y. Chen, Preparation of magnetic indole-3- acetic acid imprinted polymer beads with 4-vinylpyridine and β-cyclodextrin as binary monomer via microwave heating initiated polymerization and their application to trace analysis of auxins in plant tissues, J. Chromatogr. A, 1217 (2010) 7337-7344.

[30] C. Xu, K. Xu, H. Gu, R. Zheng, H. Liu, X. Zhang, Dopamine as A Robust Anchor to Immobilize Functional Molecules on the Iron Oxide Shell of Magnetic Nanoparticles, J. Am. Chem. Soc, 126 (2004) 9938-9939.

[31] W. S. Hummers Jr and R. E. Offeman, Preparation of Graphitic Oxide, J. Am. Chem. Soc, 80 (1958) 1339.

[32] T. Jing, H. Xia, Q. Guan, W. Lu, Y. Zhou, S. Mei, Rapid and selective determination of urinary lysozyme based on magnetic molecularly imprinted polymers extraction followed by chemiluminescence detection, Anal. Chim. Acta, 692 (2011) 73-79.

[33] B. Sellergren, Polymer- and template-related factors influencing the efficiency in molecularly imprinted solid-phase extractions, Trends. Anal. Chem, 18 (1999)

164-74.

- A CL biosensor for Lys was obtained coupled with SMIP based on ILs-Fe_3O_4@DA/GO/β-CD
- Absorption capacity of ILs-Fe_3O_4@DA/GO/β-CD-SMIP to Lys reached up to 101 mg/g
- The adsorption equilibrium was reached within 10 min
- Adsorption model followed Langmuir isotherm
- The CL system was luminol, $K_3[Fe(CN)_6]$ and NaOH solutions